Infinite compressibility states in the Hierarchical Reference Theory of fluids. II. Numerical evidence

Albert Reiner* and Gerhard Kahl
Institut für Theoretische Physik and Center for Computational Materials Science, Technische Universität Wien, Wiedner Hauptstraße 8–10, A–1040 Vienna, Austria.
**e-mail:* areiner@tph.tuwien.ac.at

Continuing our investigation into the Hierarchical Reference Theory of fluids for thermodynamic states of infinite isothermal compressibility κ_T we now turn to the available numerical evidence to elucidate the character of the partial differential equation: Of the three scenarios identified previously, only the assumption of the equations turning stiff when building up the divergence of κ_T allows for a satisfactory interpretation of the data. In addition to the asymptotic regime where the arguments of part I directly apply, a similar mechanism is identified that gives rise to transient stiffness at intermediate cutoff for low enough temperature. Heuristic arguments point to a connection between the form of the Fourier transform of the perturbational part of the interaction potential and the cutoff where finite difference approximations of the differential equation cease to be applicable, and they highlight the rather special standing of the hard-core Yukawa potential as regards the severity of the computational difficulties.

Keywords: liquid-vapor transitions, non-linear partial differential equations, numerical analysis, finite differences, stiffness

I. INTRODUCTION

In part I [1] of the present series of reports aiming at a characterization of the asymptotic solution of the Hierarchical Reference Theory (HRT, [2–8]) partial differential equation (PDE) for thermodynamic states of diverging isothermal compressibility κ_T a total of three different scenarios have been identified. Sticking to the notational conventions and the definitions introduced in part I, its appendix in particular, these are conveniently distinguished by the values of the exponents r and s in the relations

$$\begin{aligned} \frac{\partial f}{\partial Q} &= \mathbf{O}(\bar{\varepsilon}^s), \\ \frac{\partial^2 f}{\partial \varrho^2} &= \mathbf{O}(\bar{\varepsilon}^r) \end{aligned} \tag{1}$$

assumed to hold for large $\bar{\varepsilon} \equiv \varepsilon - 1$, which itself is essentially the exponential of $f(Q, \varrho)$. The latter is an auxiliary quantity related to the first derivative of the free energy at density ϱ with respect to the renormalization group theoretical cutoff wavenumber Q. Its evolution is governed by a quasi-linear PDE of the form

$$\frac{\partial f}{\partial Q} = d_{00} + d_{02}\,\frac{\partial^2 f}{\partial \varrho^2}, \qquad d_{0i} = \mathbf{O}(\bar{\varepsilon}); \tag{2}$$

in case $\bar{\varepsilon}$ acquires a power-law dependence on Q these orders of the d_{0i} are no longer valid and require some modifications that can be found in section V of part I [1]. Integration of the above PDE proceeds from $Q = \infty$ all the way to $Q = 0$, thus mirroring the transition from the hard spheres of diameter σ serving as reference system, $v^{(\infty)}(r) \equiv v^{\mathrm{hs}}(r)$, to the physically relevant target system with potential $v^{(0)}(r) \equiv v(r) = v^{\mathrm{hs}}(r) + w(r)$. At intermediate Q the cutoff dependent potential $v^{(Q)}(r)$ bears little resemblance to $v(r)$ [9] and should be regarded as a purely formal device. Its precise definition can be found in part I [1], together with that of f, $\bar{\varepsilon}$, the PDE coefficients d_{0i}, and of any further symbols not explicitly introduced.

According to eq. (A6) of part I [1] the isothermal compressibility κ_T of the target system is proportional to $\bar{\varepsilon}$ at $Q = 0$ so that infinite compressibility at the critical point and within the binodal directly implies a singular limit of $f(Q, \varrho)$ as $Q \to 0$. The boundaries of the density range of diverging f are naturally identified with the densities ϱ_v and ϱ_l of the coexisting vapor and liquid phase. Outside the interval $[\varrho_v, \varrho_l]$ as well as for non-vanishing cutoff at arbitrary density, the solution $f(Q, \varrho)$ of eq. (2) is guaranteed to be continuous and differentiable by construction. As we have seen in part I [1], the conditions of continuity, of occurrence of a singularity, and of finiteness allow us to extract a great deal of information from the HRT PDE. Of course, it is the initial and boundary conditions imposed upon f that uniquely determine the solution of the PDE throughout its domain $\mathcal{D}$ and so select which of the three types of asymptotic solutions we identified are realized in actual calculations.

The most natural assumption is, of course, that $f(Q, \varrho)$ remains smooth even for $Q \to 0$ and $\bar{\varepsilon} \to \infty$, corresponding to $r = s = 0$; smoothness as we understand it is tantamount to an $\bar{\varepsilon}$ independence of the Q and ϱ scales characteristic of the variation of f, *cf.* eq. (1). As discussed in section III of part I [1], the strongest arguments in favor of this simplistic smoothness assumption are the intuitive appeal of the mechanism sketched there and the prediction $f \propto 1/Q$, immediately implying $r = s = 0$, of the detailed analysis of ref. 7. These values of the exponents are, however, not easily reconciled with eq. (1) and the asymptotic scaling of the coefficients d_{0i} for large

$\bar{\varepsilon}$ indicated in eq. (2): Mathematical consistency can be maintained in this scenario only by invoking the possibility of a cancellation of terms that does, however, pose rather stringent conditions we have not been able to confirm from the properties of the coefficient functions, *cf.* section III of part I [1].

The other extreme, discussed in section VI of part I [1], is described by exponents $r > 0$ and $s > 1$: In this case the PDE turns stiff in that part of the integration domain $\mathcal{D}$ where $\bar{\varepsilon}$ is large, and the solution there is characterized by rapid low-amplitude oscillations around the rather slowly varying, large mean value of f. In numerical calculations on discretization grids that maintain a finite separation of the mesh points even as f and $\bar{\varepsilon}$ diverge, however, these oscillations can neither be followed nor adequately represented. The solution of the finite difference (FD) approximation of the PDE is therefore bound to reproduce vanishing effective exponents r_{eff} and s_{eff}. Smoothness so having been restored, if only as an artifact of the computational scheme, the arguments of section III B of ref. 7 naturally apply so that $f \propto 1/Q$ is to be expected again numerically even though the markedly non-smooth exact solution of the PDE is likely to display a stronger singularity, *cf.* sections VI and VII of part I [1].

In addition to the two scenarios sketched above, referred to as the simplistic, or genuinely smooth one ($r = s = 0$) and the stiff, or only effectively smooth one ($r > r_{\text{eff}} = 0$, $s > 1$, $s_{\text{eff}} = 0$), respectively, there is also the third possibility of a monotonous growth not necessarily affected by cancellation: As discussed in section V of part I [1], this implies only a very weak, *viz.*, logarithmic divergence of f for $Q \to 0$ that is compatible with a small range of values for the exponents r and s. At any rate, it can be shown that $\bar{\varepsilon}\,Q^2$ tends to a finite limit for $Q \to 0$. As we will see in section II, however, the numerical evidence clearly rules out this possibility.

It is thus only the simplistic and the stiff scenarios that remain to be considered in the bulk of this report in our attempt to elucidate the true character of the asymptotic solution of the PDE for infinite κ_T. To this end we employ an unconditionally stable implicit predictor-corrector scheme shortly outlined in section III A. A more extensive discussion of the implementation can be found in refs. 10, 11, where default settings for the most important customization parameters are also documented, and further technical information is available with the source distribution itself [12]. We illustrate the types of behavior encountered in practical calculations by taking recourse to two simple model potentials $v(r) = v^{\text{hs}}(r) + w(r)$, *viz.*, to the hard-core Yukawa (HCY) system,

$$w^{\text{hcy}}(r) = \begin{cases} -\epsilon_0 & : \; r < \sigma \\ -\epsilon\,\frac{\sigma}{r}\,e^{-z\,(r-\sigma)} & : \; r > \sigma, \end{cases} \tag{3}$$

and to square wells (SWS),

$$w^{\text{sw}}(r) = \begin{cases} -\epsilon & : \; r < \lambda\,\sigma \\ 0 & : \; r > \lambda\,\sigma. \end{cases} \tag{4}$$

In both of these potentials, ϵ coincides with the negative of the contact value of the interaction, $\lim_{r\to\sigma+}\,(-w(r))$, and so sets the energy scale of the problem. The potential range is given by $1/z$ and $\lambda\,\sigma$, respectively. Unless stated otherwise, ϵ_0, the value of $w^{\text{hcy}}(r)$ inside the core, coincides with ϵ, a choice shared with the implementation by the authors of HRT and their coworkers referred to as the original one in refs. 10, 11, *q. v.*. A short summary of the parameter sets and of the sample isotherms considered in this study can be found in tab. I.

The results of the computations reported in section III do, indeed, allow us to infer the character of the PDE for subcritical temperatures, $T < T_c$, with great confidence, if only indirectly due to the great computational similarity of genuine and effective smoothness. Our main evidence in favor of the stiff scenario derives from the rather detailed and testable predictions it entails, all of which are confirmed numerically. By way of contrast, the simplistic scenario does not hold an explanation for the observed trends, especially as regards the dependence of the FD results on the properties of the discretization grids.

Our conclusion that the PDE actually turns stiff in part of $\mathcal{D}$ for $T \le T_c$ then paves the way for some purely heuristic arguments relating the onset of smoothing in Q to the form of the Fourier transform of the perturbational part of the potential (section IV). So having understood the behavior of the PDE in the limit $Q \to 0$ where asymptotic reasoning valid for large $\bar{\varepsilon}$ applies, in section V we then turn to similar computationally problematic features of its solution at much higher cutoff where the numerical evidence points to a mechanism not unlike that at work in the asymptotic region. We close with an informal discussion of the reasons for the atypical computational properties of HCY fluids of moderate inverse screening length z (section VI), postponing practical application of the insight into the solution of the discretized PDE gained thus far to later installments of this series of reports [13].

II. THE MONOTONICITY ASSUMPTION REFUTED

Of the three scenarios put forward in part I [1] and touched upon in the introduction, the one mentioned last differs markedly from the other two in that the assumption of a merely logarithmic divergence of f furnishes the rather specific prediction of $\bar{\varepsilon}\,Q^2$ tending to a finite limit for $Q \to 0$. Of course, the possiblity of non-zero s means that, in principle, the smoothing effect discussed in section VI of part I [1] must be reckoned with. The singularity being so mild, however, a possible reduction of $s > 0$ to an effective value of $s_{\text{eff}} = 0$ is preempted by the choice of step sizes ΔQ:

In our implementation of the theory the cutoff in the i^{th} FD step is parametrized as

$$Q_{(i)} = \ln\left(e^{a - i\,b} + 1\right), \qquad i = 0, 1, \ldots,$$

as is the case for the program the original authors of HRT and their coworkers employ, too. Here a is close to the cutoff $Q_{(0)} \equiv Q_\infty$ where initial conditions are imposed on f, and b is the spacing $\Delta Q\big|_\infty$ of successive cutoffs in the large Q limit. For small Q we have to consider $i \to \infty$: The exponential $e^{a-i\,b}$ then being small, we can apply the first-order expansion $\ln(1+x) = x + \mathbf{O}(x^2)$ to obtain $Q_{(i)} \approx e^{a-i\,b}$; the step size in Q is then given by

$$Q_{(i+1)} - Q_{(i)} \approx -Q_{(i)}\,\left(1 - e^{-b}\right), \qquad Q_{(i)}\,\sigma \ll 1,$$

which is proportional to the cutoff under consideration, $\Delta Q \propto Q$. If $\bar{\varepsilon}\,Q^2$ is to approach zero or a finite constant as predicted by the assumption of monotonous growth these step sizes thus turn out of order $\mathbf{O}(\bar{\varepsilon}^{-1/2})$ at most, and our discretization should allow us to follow the variation of f reasonably well all the way to $Q = 0$. From fig. 1, however, we see that $\bar{\varepsilon}\,Q^2$ clearly diverges for $Q \to 0$. As this finding is corroborated by further calculations with a smaller setting of the numerical parameter $\Delta Q\big|_\infty$, on finer density grids (down to $\Delta\varrho = 5{\cdot}10^{-4}/\sigma^3$), and for both hard-core Yukawa and square well potentials we feel we can safely exclude the monotonous growth scenario from further consideration.

III. SMOOTHNESS *VS.* STIFFNESS

As for the remaining two alternatives, an attempt to distinguish numerically between genuine and effective smoothness seems doomed at first sight. And indeed, fig. 2 shows the small Q behavior of f within the binodal as obtained numerically to be in excellent agreement with $f \propto 1/Q$, and figs. 2, 3, and 5 as well as the numerical data demonstrate that f is of the form postulated in part I [1], *q. v.*. Both of these observations fit the simplistic scenario just as well as the stiff one. Nevertheless, close scrutiny of the computational process and the numerical results yields a wealth of indirect evidence that we feel is sufficient to establish the character of the PDE for $T < T_c$ with great confidence, if not with absolute certainty. Of course, since the solution $f(Q,\varrho)$ is computationally smooth in either case, the simplistic scenario can never be ruled out altogether as smoothness is its sole defining property. Instead, we base our reasoning on the rather specific, and numerically testable predictions that follow from the assumption of stiffness of the PDE and stand in marked contrast to the expectations furnished by the simplistic scenario. As we will show in this section, it is the assumption of a stiff PDE that is in full accordance with the numerical findings whereas smoothness is only marginally compatible with some of their traits, especially as regards the SW data.

Before going into the details of the vastly different consequences of the two scenarios, it is worthwhile to step back for a moment and ask why we have to adopt the eq. (2) in the first place if the most direct formulation of the theory is that of a PDE for the free energy $A^{(Q)}(\varrho)$ of the Q system at density ϱ, *cf.* part I [1]. Indeed, from eqs. (A2) and (A3) of part I [1] we see that $\partial A^{(Q)}/\partial Q \propto Q^2\,(f + \text{const})$ for $Q\,\sigma \ll 1$, so that the Q and ϱ scales characteristic of $A^{(Q)}(\varrho)$ are essentially the same as those appropriate for $f(Q,\varrho)$. In the smooth scenario there is then no reason for the formulation in terms of f to be preferable to that in terms of the free energy, provided proper care is taken to ensure stability and convergence. This has certainly been the case in our earlier work shortly summarized in appendix B.1 of ref. 11 that nevertheless was unable to proceed to small Q for $T < T_c$. Similar difficulties are reported in ref. 6, and indeed to the best of our knowledge there are no HRT results on simple one-component fluids for $T < T_c$ except in the quasilinear formulation of eq. (2) or variants thereof. — In the stiff scenario all this is, of course, to be expected as the rapid low amplitude oscillations of the solution in this case necessitate step sizes that are reduced as some inverse power of $\bar{\varepsilon}$ or the exponential of $\partial A^{(Q)}/\partial Q$, and only under special circumstances do the discretized equations allow one to obtain a solution with the much larger step sizes used in practical applications. As noted in section II of part I [1], the auxiliary quantity $f(Q,\varrho)$ was introduced exactly for this reason [8].

As discussed in section VI of part I [1], if the PDE becomes stiff in part of $\mathcal{D}$ the onset of smoothing may involve either of two mechanisms, depending on whether the step sizes ΔQ or $\Delta\varrho$ become inadequate first. Not surprisingly, the two possible orderings for the cutoffs $Q_{\Delta Q}$ and $Q_{\Delta\varrho}$ assigned in an interpretation of the numerical results in terms of the stiff scenario entail vastly different consequences and are therefore discussed separately in subsections III B ($Q_{\Delta\varrho} > Q_{\Delta Q}$) and III C ($Q_{\Delta Q} > Q_{\Delta\varrho}$) below.

Before that, however, some general remarks are in place: Letting the labels x and y refer to either Q or ϱ, in the stiff scenario smoothing in x sets in at $Q = Q_{\Delta x}$ and can always be postponed, *i. e.*, shifted to lower cutoffs by decreasing the step size Δx. If, however, the corresponding exponent, r or s, is positive, the rapid growth of f, $\bar{\varepsilon}$ and, by way of eq. (1), of $|\partial^2 f/\partial x^2|$ as the solution proceeds towards $Q = 0$ implies that the amount by which $Q_{\Delta x}$ can be changed in this way and the attendant computational effects must be small. For positive exponents the $Q_{\Delta x}$ are thus fairly well defined despite the gradual nature of the transition to the smoothing regime. — Furthermore, without loss of generality assuming $Q_{\Delta x} > Q_{\Delta y}$, $Q_{\Delta x}$ is obviously independent of the step sizes Δy. The solution obtained numerically at cutoffs below $Q_{\text{smooth}} \equiv Q_{\Delta x}$ is already affected by smoothing in x so that there is no point in identifying $Q_{\Delta y}$ with the cutoff where Δy becomes too large to describe the variation of the no longer accessible true solution of the PDE. Instead, $Q_{\Delta y}$ is taken to be the cutoff where smoothing in y commences in the solution of the FD equations (FDEs), which implies a Δx dependence of $Q_{\Delta y}$ and may even induce $Q_{\Delta y}$ to vanish altogether. For $Q < Q_{\Delta y}$, the solution generated numerically by neces-

sity conforms to the simplistic smoothness assumption as $r_{\text{eff}} = s_{\text{eff}} = 0$ and so grows like $1/Q$ in a stable manner. This proportionality also means that the form of f for $\varrho_1 < \varrho < \varrho_2$ remains constant from $Q_{\Delta y}$ all the way to the final results at zero cutoff. (Here and below the form of f at some cutoff Q refers to $f(Q, \varrho)$ as a function of ϱ without regard for the overall normalization of f.) — The important mechanism sketched in section III of part I [1] and the concomitant stabilization of form and monotonicity of f do not explicitly depend on s and thus always set in at $Q_{\Delta\varrho}$; incidentally, figs. 2 and 3 show its preconditions, *viz.*, flatness and compatibility with the sketch of part I [1] to be met numerically. Of course, both $Q_{\Delta Q}$ and $Q_{\Delta\varrho}$ depend on temperature and density, which is taken to be silently accounted for whenever we speak of the form of f at one of the $Q_{\Delta x}$, and they are defined only in that part of $\mathcal{D}$ where f is large.

A. Numerical aspects

As some of the numerical effects are rather subtle, we should also recall several key aspects of the implementation we rely on. This is a highly flexible and fully modular computational framework for the solution of a FD approximation of the PDE by an implicit predictor-corrector scheme thoroughly discussed in refs. 10, 11. For consistency with eq. (2), in the calculations reported in the present contribution we refrain from implementing the core condition. The discretization is applied on uniform density grids and with the predetermined step sizes ΔQ of section II. Convergence of the FD equations has been checked, and iteration of the corrector step does not bring about noticeable changes.

In practical applications, the discretized equations generally cannot be solved down to arbitrarily small Q for $T < T_c$, and the smallest cutoff reached we denote $Q_{\min}$. As the failure modes responsible for an end of the program are known [10, 11] and can be linked to the local behavior of the solution, *v. i.*, the systematic changes in $Q_{\min}$ upon variation of aspects of the numerical procedure prove a powerful and readily accessible diagnostic tool. For the calculations reported here, the immediate cause for abortion of the computation at some cutoff $Q_{\min}$ is either an insufficient adaptation of the rescaling necessary for representing quantities affected by exponentiation of f — the scale of fig. 1 alone shows that, *e. g.*, $\bar{\varepsilon}$ cannot be represented in double precision — or else because of non-real f and negative $\varepsilon \equiv \bar{\varepsilon} + 1$ in the predictor step. These two effects are linked to pronounced increase and decrease of f, respectively.

Unlike the $Q_{\Delta x}$, $Q_{\min}$ obviously does not depend on the density. Instead, it is essentially determined by the physical potential $w(r)$, the temperature, the discretization grid, and the formulation of the theory [10]. As for the latter, if the PDE is coupled to further constraints, and the solution vector augmented by additional components to be determined accordingly, the likelihood of an early termination of the computation in the predictor step generally increases, and so does $Q_{\min}$. As the customary manner of implementing the core condition involves an expansion of the direct correlation function inside the core [6, 10], the sensitivity of $Q_{\min}$ to an increase in N_{cc}, the number of expansion coefficients, again proves of interest.

With this rough sketch of some of the salient features of the computational process — more detail can be found in refs. 10, 11 and with the source code distribution [12] — we are now ready for a detailed look at some numerical results obtained for two model systems, *viz.*, the HCY and SW fluids exemplifying the cases $Q_{\Delta\varrho} > Q_{\Delta Q}$ and $Q_{\Delta Q} > Q_{\Delta\varrho}$, respectively.

B. Smoothing in ϱ first

So let us first turn to the HCY fluid of inverse screening length $z = 1.8/\sigma$ already considered in ref. 10. As mentioned before, the numerical solution must be smooth at any rate and is therefore compatible with the simplistic scenario. For a genuinely smooth solution, however, we expect only a small dependence of the results on ΔQ and $\Delta\varrho$ that should be essentially stochastic in nature, stemming from the truncation error in an otherwise unproblematic FD approximation of the PDE alone.

As we shall see in a moment, the numerics can also be reconciled with the stiff scenario if only we assume smoothing to occur in the ϱ direction first, $Q_{\Delta\varrho} > Q_{\Delta Q}$. In this case the mechanism responsible for stable growth of f (*cf.* section III of part I [1]) is at work at all cutoffs below Q_{smooth}. As an immediate consequence, the stability of the computational process is not an issue, and incorporation of the core condition is entirely unproblematic. An overflow due to an insufficient adaptation of the re-scaling of non-$\mathbf{O}(1)$ quantities, *v. s.*, is the only possibility for numerical failure. The likelihood of this is greatly reduced when ΔQ is decreased so that smaller step sizes are generally accompanied by smaller values of $Q_{\min}$. A systematic $\Delta\varrho$ dependence of $Q_{\min}$ is not anticipated. — For a fixed density grid, we infer the following characteristics of the ΔQ dependence of the results: First of all, $Q_{\Delta\varrho}$ exceeds $Q_{\Delta Q}$ and so cannot depend on ΔQ, nor can f at $Q_{\Delta\varrho}$. On the other hand, even though smaller step sizes (in our implementation determined by the parameter $\Delta Q\big|_\infty$, *cf.* section II) correspond to smaller $Q_{\Delta Q}$, the large value of the exponent $s > 1 > 0$ implies that the drop in $Q_{\Delta Q}$ must be exceedingly small. As furthermore the evolution from $Q_{\Delta\varrho}$ down to $Q_{\Delta Q}$ is determined by the solution at the onset of smoothing and the properties of only the density grid, the form of f below $Q_{\Delta Q}$ is virtually ΔQ independent. — As for a variation of the density grid at fixed ΔQ, a reduction of $\Delta\varrho$ clearly entails a shift of $Q_{\text{smooth}} \equiv Q_{\Delta\varrho}$ to smaller cutoffs, which may in turn cause a change in $Q_{\Delta Q}$, too. These effects must be rather small because of the non-zero exponenets r and s, and they must vary

with the density for the same reason the $Q_{\Delta x}$ are density dependent. A change of the ϱ grid thus implies a small change of the form of f at $Q_{\Delta\varrho}$ and, hence, at $Q_{\Delta Q}$ and all smaller cutoffs. As long as $Q_{\Delta\varrho}$ does not fall below $Q_{\Delta Q}$, however, the ratio of the forms of f as obtained on different discretization grids cannot depend on ΔQ.

As conformance with the simplistic scenario is certain anyway, it remains to be seen to what degree the detailed predictions of the stiff one are fulfilled in actual computations. To this end, in tabs. II to IV we summarize the numerical results for a HCY potential with $z = 1.8/\sigma$ obtained on density grids with $\Delta\varrho = 10^{-2}/\sigma^3$ and $\Delta\varrho = 5 \cdot 10^{-4}/\sigma^3$ and varying ΔQ. For fixed density grid (tabs. II and III, respectively), $Q_{\min}$ and, hence, the final values of f markedly depend on ΔQ, the former generally decreasing and the latter increasing upon reduction of the step size. On the other hand, both the form of f and its magnitude at fixed cutoff — to be found in the tables under the headings of F_x^y and $f_x\, Q_{\min}\, \sigma$, respectively — remain largely unchanged. Comparing the results obtained with different settings for $\Delta\varrho$, the change in the final values of f is indeed almost completely due to the differences in $Q_{\min}$. The magnitude at fixed Q, on the other hand, is affected only moderately, *viz.*, by a few per cent for a twenty-fold increase in the density resolution, and it depends on ϱ but not on ΔQ, *cf.* tab. IV. $Q_{\min}$ itself is not affected by the density grid in a systematic way. Of the two sample isotherms that founder at comparatively large cutoff $Q_{\min}$, *viz.*, the ones at $\Delta Q\big|_\infty = 0.003/\sigma^3$, $\Delta\varrho = 10^{-2}/\sigma^3$ and at $\Delta Q\big|_\infty = 0.004/\sigma^3$, $\Delta\varrho = 5 \cdot 10^{-4}/\sigma^3$, only the former does not enter the asymptotic regime where $f \propto 1/Q$, as can clearly be seen from tab. IV. All in all, the numerical results are in excellent agreement with stiffness, and we note that for this system and the density grids considered $Q_{\Delta Q}$ must be sought around $10^{-2}/\sigma$.

C. Smoothing in Q first

In our previous work on HRT [10, 14] we repeatedly stressed the vastly different numerical properties of the HCY and SW potentials. This is certainly not anticipated on the basis of the simplistic scenario that furnishes only the same prediction of a small discretization grid dependence well explained by the truncation error as for the HCY system. Still, the assumption of a genuinely smooth solution is certainly compatible with the numerics, if only marginally so in the face of the most prominent feature of the evolution of f, *viz.*, episodes of much more rapid variation than mere proportionality to $1/Q$.

Assuming the PDE to turn stiff for large f instead, and furthermore $Q_{\Delta Q}$ to exceed $Q_{\Delta\varrho}$ for the present system, there is a Q range $Q_{\Delta\varrho} < Q < Q_{\Delta Q}$ where FDEs are used with inappropriately large step sizes ΔQ while oscillations in ϱ are not yet suppressed. For these cutoffs, the stabilization wrought by the mechanism of growth first introduced in section III of part I [1] is not effective yet, and there is no reason for f to be convex from below throughout the density range $\varrho_1 < \varrho < \varrho_2$. On the other hand, the overall profile of f is expected to resemble fig. 1 of part I [1], and $s_{\text{eff}} = 0$ once more suggests a general growth proportional to $1/Q$. The sign of $\partial^2 f/\partial\varrho^2$ is thus unconstrained, and its modulus increases in unison with f, *i. e.*, in proportion to $1/Q$. As d_{00}/d_{02} is of order $\mathbf{O}(1)$ in $\bar{\varepsilon}$, however, the $\mathbf{O}(1)$ growth of $\partial^2 f/\partial\varrho^2$ may well be sufficient to destabilize the mechanism of growth discussed in section III of part I [1] at some $Q \in (Q_{\Delta\varrho}, Q_{\Delta Q})$, and so give rise to a much more rapid variation of f as a function of Q. Of course, these near-discontinuities of f will occur at different cutoffs for different densities, most often close to the edges ϱ_1 and ϱ_2 of the region of large f where the $Q_{\Delta x}$ are smallest, and neighboring densities will experience them at roughly the same cutoff. Furthermore, in principle the jumps should lead to both increases and decreases in f, depending on the sign of $\partial^2 f/\partial\varrho^2$ at slightly larger Q. Considering the numerics, however, a large change in f is almost certain to bring the calculation to an end, and all the failure modes discussed in section III A are relevant for $Q_{\min}$. A comparatively mild increase of f, on the other hand, may relax the relative curvature of f to the point of allowing the solution to enter once more an episode of near-stability characterized by growth in approximate proportion to $1/Q$. As for an incorporation of the core condition, in accordance with section III A the attendant introduction of additional degrees of freedom is likely to exacerbate the risk of triggering such a jump in f, *cf.* section V. — To understand the grid dependence of the numerics under the assumption of stiffness, recall that $Q_{\min}$ itself is the location of a failed jump in f. As smoothing in Q is the driving force behind the computational process, $Q_{\min}$ must be quite sensitive to ΔQ, but there is no reason for $Q_{\min}$ to be monotonous in ΔQ. The density grid, on the other hand, is still adequate for the elliptic boundary value problem in ϱ at constant Q. If the numerical process were stable, there should thus be no appreciable dependence of the results on $\Delta\varrho$ at all. In the absence of the stabilization wrought by smoothing in ϱ, however, even the small differences seen upon variation of $\Delta\varrho$ must be expected to shift the episodes of rapid evolution to slightly different cutoffs in an unsystematic way. By the same token, the $\Delta\varrho$ dependence of the final form of f should be small, and different ΔQ should leave it unaltered as long as the number and the approximate positions of the jumps do not change. As those are least frequent close to the maximum of f, its form is expected to be most stable in the central part of the density interval of large f.

In tabs. V and VI we summarize the numerical results for a SW potential of range $\lambda = 3$ obtained on the same discretization grids as the HCY data of section III B. Of course, the numerics cannot be in contradiction with the simplistic scenario. As for the consequences of stiffness, the most prominent feature predicted concerns the occurrence of near-discontinuities of the solution of the FDEs.

These jumps are, indeed, to be found in the data underlying fig. 3 at the positions marked with arrows, and several of them can be seen clearly even on the logarithmic scale of the graph. All the other expectations following from the stiff scenario with $Q_{\Delta Q} > Q_{\Delta\varrho}$ also compare well with the data of tabs. V and VI: In particular, a pronounced ΔQ dependence of $Q_{\min}$ is accompanied by only a very modest effect as $\Delta\varrho$ is varied, even though the relative change in $\Delta\varrho$ is much larger than that in ΔQ. Excluding the pathological data with negative f (*v. i.*), the final forms of f are mostly ΔQ independent, and the forms obtained on the two density grids differ but slightly. Only the isotherm with $\Delta Q\big|_\infty = 0.010/\sigma$ in tab. VI presents a somewhat different shape than those at smaller $\Delta Q\big|_\infty$. The differences in the numbers given under the heading F_x^y are, however, still in accordance with the stiff scenario as discrepancies appear only close to the edge of the density range of large f. As for the first entry of tab. V ($\Delta Q\big|_\infty = 0.003/\sigma$), negative f corresponds to exceedingly small values of $\varepsilon \equiv \bar{\varepsilon} + 1 \sim 10^{-27}$. This is found to be the result of a downward jump from $f \sim +10^4$ ($\varepsilon \sim 10^{5000}$) at only slightly higher cutoff where the form of f again corresponds to that of the other isotherms. Clearly, even a minor perturbation of the numerical process might easily have led to negative ε and hence to a numerical exception; in this case our implementation would have discarded the last step, and the final results would once more conform with those of the remainder of tab. V.

Let us shortly return once more to the most salient feature of the numerical solution, *viz.*, its near-discontinuities. Disregarding the analytical considerations of part I [1] it might be tempting to imagine that, for $T < T_c$, the PDE generates a shock front approximately symmetrically moving outward towards the densities ϱ_v and ϱ_l of the coexisting phases as Q approaches zero. In this view of the numerical process the jumps occur when the shock reaches the corresponding density. Such an interpretation is not consistent with the data: According to fig. 3 the near-discontinuities of f occur repeatedly at the same density (most conspicuously for $\varrho = 0.1/\sigma^3$), and rapid change at one density is generally accompanied by similar behavior at other densities. Neither of these observations is compatible with the idea of a moving shock front, nor is there any reason why the binodal should be linked to a shock front in SWs but not in the HCY fluid, *cf.* section III B.

D. Assertion of stiffness

Summarizing the numerical evidence presented so far we find that of the three scenarios found in part I [1] only the possibility of a merely logarithmic singularity of f can be ruled out with certainty. We are then faced with the two alternatives of genuine smoothness of the PDE on the one hand, and effective smoothness as a result of an FD approximation to a stiff PDE on the other hand. As shown in the preceding subsections III B and III C, neither of them is in direct contradiction with the numerical data.

The crucial difference is their respective specificity and testability: The simplistic scenario does not make any predictions beyond the smallness of the discretization grid dependence of the numerical results, nor does it offer any of the detailed understanding of the computational process that is necessary for accurate and reliable interpretation of the FD results. By way of contrast, stiffness of the PDE in part of its domain provides a consistent framework for the interpretation of the numerics and furthermore entails a number of concrete and numerically testable consequences, all of which are in excellent agreement with our data once the correct ordering of the $Q_{\Delta x}$ has been chosen. In combination with the analytical considerations of part I [1] and our earlier statements regarding the importance of the formulation of the HRT PDE employed, the specificity and great number of these predictions provide ample, although necessarily indirect evidence in favor of the stiff scenario.

From this point on we will therefore take it for granted that the HRT PDE does, indeed, turn stiff in part of its domain for subcritical temperatures. On this basis we now aim to further enhance our understanding of the HRT numerics in the remainder of this report, shedding some light on the location of $Q_{\Delta Q}$ (section IV), extending our findings in the asymptotic region to intermediate Q (section V), and finally clarifying the outstanding numerical properties of the HCY potential *vis-à-vis* other physical systems (section VI).

IV. THE ONSET OF SMOOTHING IN Q

If our view of the underlying PDE and the numerical process is correct, it is natural to inquire into the typical values of the cutoffs $Q_{\Delta x}$ where smoothing in x sets in. As the exponents r and s are non-zero by assumption, these cutoffs may only weakly depend on the discretization grid and so are largely determined by the perturbational part of the potential alone. As far as $Q_{\Delta\varrho}$ is concerned, we are currently in no position to even tentatively predict its location from the properties of the model system under consideration. For smoothing in Q, on the other hand, we now present some purely heuristic arguments that shed some light on the factors that influence the value of $Q_{\Delta Q}$ by relating the likelihood of finding it at some cutoff to the form of the Fourier transform $\tilde{w}(k)$.

In order to extract a likely position of $Q_{\Delta Q}$ from the PDE we consider a thermodynamic state of diverging isothermal compressibility at a cutoff that is low enough for smoothing in Q to have set in at least partially, $Q \lesssim Q_{\Delta Q}$: In view of the gradual transition between the smoothing and non-smoothing regimes, the effective exponent s_{eff} may not vanish exactly yet; nevertheless it seems safe to assume $s_{\text{eff}} < 1$. Let us now define an

auxiliary quantity $\psi(Q,\varrho)$ through the relation

$$\tilde{\mathcal{K}} + \psi\,\tilde{u}_0 = -\frac{\tilde{\phi}}{\bar{\varepsilon}}. \tag{5}$$

In the notation of our earlier work on HRT [1, 10, 11, 14] ψ corresponds to $\tilde{\phi}_0 + \gamma_0$, where γ_0 is an expansion coefficient in the direct correlation function used to enforce thermodynamic consistency in the form of eq. (A5) of part I [1]. Solving the above relation for ψ and differentiating once with respect to Q we find

$$\frac{\partial\psi}{\partial Q} = -\tilde{\phi}_0\left(\frac{\partial}{\partial Q}\frac{1}{\bar{\varepsilon}} + \frac{\partial}{\partial Q}\frac{\tilde{\mathcal{K}}}{\tilde{\phi}}\right),$$

which is valid at all cutoffs except close to the zeros $Q_{\tilde{\phi},i}$ of $\tilde{\phi}$ and $\tilde{u}_0$ where eq. (5) cannot be inverted to yield ψ. As shown in section 2.4.1 of ref. 11, the compressibility sum-rule also allows one to derive a PDE for γ_0 that is equivalent to eq. (2) itself. Taking into account the density independence of the potential we easily find that the evolution of ψ is given by

$$\begin{aligned}\frac{\partial\psi}{\partial Q} &= -\frac{Q^2}{4\,\pi^2}\,\frac{\partial^2}{\partial\varrho^2}\ln\varepsilon \\ &= \frac{Q^2}{4\,\pi^2}\left(-\tilde{u}_0^2\,\frac{\partial^2 f}{\partial\varrho^2} + \tilde{\phi}\,\frac{\partial^2}{\partial\varrho^2}\frac{1}{\tilde{\mathcal{K}}}\right).\end{aligned}$$

Equating the two expressions for $\partial\psi/\partial Q$ we can now solve for $\partial^2 f/\partial\varrho^2$ and insert the result into the PDE (2) to obtain the rate of change of f as

$$\frac{\partial f}{\partial Q} = d_{00} + \frac{d_{02}\,4\pi^2}{Q^2\,\tilde{u}_0^2}\left(\tilde{\phi}_0\,\frac{\partial}{\partial Q}\frac{1}{\bar{\varepsilon}} + \frac{\partial}{\partial Q}\frac{\tilde{\mathcal{K}}}{\tilde{u}_0}\right) + \frac{d_{02}\,\tilde{\phi}_0}{\tilde{u}_0}\,\frac{\partial^2}{\partial\varrho^2}\frac{1}{\tilde{\mathcal{K}}} \tag{6}$$

for Q away from the $Q_{\tilde{\phi},i}$. Of course, both d_{00} and d_{02} are negative in the case under consideration [1].

For smoothing in Q to set in we expect f to be large already, $\bar{\varepsilon} \gg f \gg 1$, or else reasoning based on the asymptotic behavior for large $\bar{\varepsilon}$ is inapplicable. Furthermore, as $Q_{\Delta x}$ is that value of the cutoff where the step sizes Δx become insufficient for representing the exact solution of the PDE, the most likely position of $Q_{\Delta Q}$ is where the slope $-\partial f/\partial Q$ of f is rather large. At the same time, for a hard-sphere reference system $Q_{\Delta Q}$ can only depend on the form of the Fourier transform of the perturbational part of the interaction potential, *i. e.*, on $\tilde{u}_0 = \tilde{\phi}/\tilde{\phi}_0$ rather than on $\tilde{\phi}$ itself: The temperature $T = 1/k_B\,\beta$ enters the calculation only as a pre-factor to the interaction potential, *viz.*, through $\phi = -\beta\,w$ so that the normalization of $\tilde{\phi}$ only fixes an energy or temperature scale.

With this in mind we return to eq. (6): Of the expressions appearing on its right hand side the one involving the Q derivative of $1/\bar{\varepsilon}$ is of order $\mathbf{O}(\bar{\varepsilon}^{s_{\text{eff}}-1})$ in $\bar{\varepsilon}$ and so can be neglected if $s_{\text{eff}} < 1$ as assumed. As we are looking for an effect triggered by the form of $\tilde{\phi}$ alone we do not have to consider the derivatives of the properties of the hard sphere reference system encoded in $\tilde{\mathcal{K}}$ either. It is then the term involving the Q derivative of $\tilde{u}_0$ that is of interest to us in the first place: The ideal gas contribution $-1/\varrho$ to $\tilde{\mathcal{K}}$ ensures positive $d_{02}\,\tilde{\mathcal{K}}$, and consequently the relevant term is the product of $\partial\tilde{u}_0/\partial Q$ and manifestly positive factors. Now assume that $Q_{\Delta Q}$ is less than the position of the first minimum of $\tilde{u}_0$ so that only the monotonous growth of $\tilde{u}_0$ towards its global maximum at $Q = 0$ remains to be covered by the solution of the PDE: Clearly, as the calculation proceeds in the negative Q direction, the steeper this rise of $\tilde{u}_0$, the more the $\partial\tilde{u}_0/\partial Q$ term counteracts the growth of f, thereby effectively further delaying the onset of smoothing in Q. Most likely, $Q_{\Delta Q}$ will thus be found at cutoffs so low that $\tilde{u}_0$ already levels off towards its limiting value of unity. Even a superficial glance at $\tilde{u}_0$ for two typical potentials, *viz.* SWs (solid curve) and the HCY system with $z = 1.8/\sigma$ (dashed curve) displayed in fig. 4 shows that, for these systems, $\tilde{u}_0$ levels off when Q (or $\lambda\,Q$, in the case of SWs) is no more than a few $10^{-1}/\sigma$. This is certainly not in contradiction to the estimate presented at the end of section III B, especially in the light of section VI below and considering the density and temperature dependence of the $Q_{\Delta x}$. Support for this view also comes from figs. 2 and 3: These demonstrate that the transition to the regime where f mostly grows like $1/Q$, corresponding to vanishing s_{eff}, occurs at similar values of the cutoff. All in all, we therefore expect that either $Q_{\Delta Q}$ is larger than the position of the first minimum of $\tilde{u}_0$, the case not considered above, or else that $Q_{\Delta Q}$ should be located at a much smaller cutoff, *viz.*, where $\tilde{u}_0$ is already close to unity and $|\mathrm{d}\tilde{u}_0/\mathrm{d}Q|$ is small. It is the latter of these possibilities that is in accordance with the data displayed in figs. 2 and 3 and the tables referenced earlier so that our arguments, heuristic as they are, do indeed seem to provide us with a means of estimating $Q_{\Delta Q}$ in a satisfactory way. Unfortunately, the location of $Q_{\Delta\varrho}$ so far eludes determination from the potential alone by a comparably simple line of thought, and actual numerical solution of the PDE currently is the only way of studying $Q_{\Delta\varrho}(T,\varrho)$ available to us.

V. BEYOND ASYMPTOTICS

On the basis of this understanding of the relation between $\tilde{w} \propto \tilde{\phi} \propto \tilde{u}_0$ and $Q_{\Delta Q}$ one might expect numerical difficulties linked to the discretization grid to first surface at about the same cutoff, *viz.*, around $Q \sim 10^{-1}/\sigma$ for the potentials considered earlier. However, the monitoring variant of our code [10–12] that must be credited with first highlighting and bringing to our attention the purported stiffness of the equations clearly signals the inadequacy of number and spacing of the vertices in the FDEs already at much higher cutoff, *viz.*, typically for $5 < Q\,\sigma < 10$: Indeed, the asymptotic region of large $\bar{\varepsilon}$ can never even be reached without renouncing control of the local truncation error in solving the equations since otherwise the step sizes appropriate in FD calculations would render the results of fixed precision floating point

operations insignificant, *cf.* section III E of ref. 10.

In combination with the observed patterns of the evolution of f at intermediate and small Q illustrated in figs. 2, 3, and 5, our experience with the numerics of HRT leads us to propose the existence of several regions of large f within $\mathcal{D}$ where phenomena similar to those discussed before are to be reckoned with: Most importantly, the variation of the exact solution of the PDE may be characterized by rapidly diminishing density and cutoff scales incompatible with a realistic discretization grid not only in the asymptotic region but also at higher cutoff. And indeed, right next to the high density boundary we see a number of patches of large f in fig. 5. Other than in part I [1], however, at intermediate Q the guarantee of continuity of f is no longer accompanied by that of its unboundedness, both of which are necessary to ensure the validity of conclusions drawn from the asymptotic behavior of the various terms in the PDE for large $\bar{\varepsilon}$ alone. The small value of $\tilde{u}_0^2$ evident from fig. 4 further complicates the situation in that $\bar{\varepsilon}$ may not be large compared to f even for $f \gg 1$. Still, from the expressions for the PDE coefficients given in part I [1] we deduce that d_{02} is negative and appreciable for all Q in the relevant cutoff range except very close to the $Q_{\tilde{\phi},i}$ where it vanishes as $\tilde{\phi}^2$, and that d_{00} is likely to be rather large in modulus for $f \gg 1$ due to the terms linear in f; for the special considerations applying to the immediate vicinity of the $Q_{\tilde{\phi},i}$, *cf.* part III [13] as well as appendix A.4 of ref. 11.

It is then conceivable that f may become large in some parts of $\mathcal{D}$ and, by way of the d_{0i} behavior there, prompt rapid further growth when Q proceeds to smaller values. As signalled by our code when monitoring the evolution of the numerical solution [10], this in turn effectively mandates either impractically small step sizes ΔQ or else deliberate resignation of bounded local truncation errors, *v. s.*. Just as in section III C, such a rapid growth of f almost certainly induces an accompanying growth of $|\partial^2 f/\partial \varrho^2|$ on the grid, and any oscillations of the density curvature will carry over to $\partial f/\partial Q$. Qualitatively the situation is then quite similar to that in the asymptotic region, and it seems reasonable to surmise that transient stiffness at intermediate cutoff might be the reason for the inability of a numerical scheme insisting on local convergence and appropriateness of the dynamically adjusted discretization mesh to ever proceed to $Q \sim Q_{\Delta x}$.

Without the backing of more formal arguments much of the above line of thought may seem insubstantial and might thus be viewed with suspicion. There are, however, a number of numerical effects that provide at least indirect evidence for the point of view just laid out. Among those we have already identified and discussed in our earlier work on HRT, the plummeting step sizes observed when determining the discretization grid from the local curvature of appropriate components of the solution vector [10, 12] are the most direct evidence in favor of stiffness of the PDE at intermediate Q. Further support comes from our study of SWs of varying range [14]: There the peculiar shifts in the critical temperature whenever λ is close to a simple fraction have been linked to the modulation of $\bar{\varepsilon}$ by the interference of $\tilde{c}_2^{\mathrm{ref}}$ and $\tilde{\phi}$; and considering our remarks on the effect of augmenting the solution vector to include new degrees of freedom beyond f (section III A), it is significant that the critical point is accessible in a wider λ range when coupling the PDE to a smaller number of expansion terms for taking into account the core condition, *cf.* section IV E of ref. 14 and appendix E of ref. 11. Assumption of transient stiffness also explains why the lowest temperature attainable numerically, denoted $1/k_B\,\beta_{\max,\#}$ in refs. 11, 14, may well be higher than T_c even though stiffness in the asymptotic region is a problem only for $T \leq T_c$, and that the isotherms show not the least sign of phase separation for $\beta < \beta_{\max,\#} < \beta_c$, the critical temperature being known independently from related computations or by other methods. — There are also some more intricate effects stemming from the interplay of the $Q_{\tilde{\phi},i}$ with the boundaries of the cutoff ranges where the step sizes ΔQ are inappropriate, as well as from the ϱ dependence of the onset of smoothing in the presence of a local density grid refinement. As the manifestations of both of these in the width of the two-phase region cannot be discussed without reference to the details of the data analysis on non-uniform high-resolution density grids they will be dealt with only in part III [13].

VI. HARD CORE YUKAWA *VS.* OTHER POTENTIALS

By now we have arrived at what we feel to be as satisfactory an understanding of the numerical process as can be expected from considerations as summary in character as those put forward in part I [1] and in the preceding section V of the present contribution: In our view, practical discretization grids are expected to cause numerical problems for low enough temperature both as the divergence of the isothermal compressibility κ_T is built up for $Q \to 0$ and at much larger cutoff when the PDE temporarily turns stiff in isolated patches of $\mathcal{D}$. Other sources of difficulties like those arising at the initial condition and the high-density boundary have been discussed extensively elsewhere [10, 11, 14].

Throughout our numerical work we consistently found that HCY fluids of moderate inverse screening length like, *e. g.*, the one with $z = 1.8/\sigma$ repeatedly used in this report as well as in ref. 10 exhibit all these phenomena only in a rather mild form. For $Q \to 0$ this is immediately clear in the stiff scenario if only we accept the in itself unexplained finding of $Q_{\Delta\varrho} > Q_{\Delta Q}$. At intermediate Q, on the other hand, the merely qualitative considerations of section V do not allow us to directly tackle the problem of clarifying the computational benignity of HCYs. Both the relative order of $Q_{\Delta Q}$ and $Q_{\Delta\varrho}$ in the asymptotic region and the comparable innocuousness of the stiffness at higher cutoff seem, however, to be linked to a specific feature of the form of the Fourier transform of the

perturbational part of the HCY interaction potential:

Once more considering fig. 4, an important difference between the HCY and SW curves is apparent right away: With the default choice of $\epsilon_0 = \epsilon$, the local extrema of the HCY $\tilde{u}_0$ at $Q > 0$ are comparatively small in modulus, as can also be seen from the numbers quoted in the caption to fig. 4. It is easily checked that the special standing of the default HCY system in this regard remains unchallenged even for other parameters and types of potentials: The main difference between SWs and other short-ranged non-HCY potentials like, *e. g.*, Lennard-Jones systems concerns the phase of the swings of $\tilde{u}_0$, *i. e.*, the location and spacing rather than the modulus of the local extrema. As for the HCY case, although an increase in z (leading to a shorter ranged potential) reduces the slope of $\tilde{u}_0$ and enhances the local extrema, the effect is quite small for moderate screening length and approaches the SW case only in the limit $z \to \infty$ that actually transforms v^{hcy} into a SW potential of vanishing well width, $\lambda = 1$.

As for the reason for $Q_{\Delta Q}$ being less than $Q_{\Delta\varrho}$, recall the decisive *rôle* in fixing $Q_{\Delta Q}$ of the steepness of $\tilde{u}_0(Q)$ as it rises towards its global maximum of unity at $Q = 0$ (section IV). A natural question is then by what standard the slope of $\tilde{u}_0$ should be judged: One possibility is, of course, its absolute value, but this requires the PDE to sense the global normalization of $\tilde{\phi}$, which is conceivable but seems rather unlikely despite the short rangedness of the potential. An intriguing alternative is to assume that it is the variation of $\tilde{u}_0$ at larger Q that sets the scale relative to which the steepness of $\tilde{u}_0$ must be assessed. Not only does this tie in well with the numerics at intermediate cutoff (*v. i.*) but it also provides a simple explanation for the particularly small value of $Q_{\Delta Q}$ in the HCY case: In relation to the undulations of $\tilde{u}_0$ at higher Q, the final growth of $\tilde{u}_0$ is particularly prominent for a HCY potential with $\epsilon_0 = \epsilon$, and the onset of smoothing in Q is postponed more effectively than, *e. g.*, in the SW case. The dependence of $\tilde{u}_0$ and, hence, of $Q_{\Delta Q}$ on λ and z then also explains the deteriorating accuracy and growing numerical problems for narrower potentials previously found for both model potential types [14, 15].

A very similar line of thought also allows us to understand the exceptional computational properties of HCY fluids at intermediate cutoff: For every one of the patches of potential stiffness including the asymptotic region there is an associated temperature below which computational problems prevent bounded local truncation errors on practical discretization grids whereas the FD equations may still admit a numerical solution. For small cutoff, these difficulties are linked to the build-up of the divergence of the isothermal compressibility, the relevant temperature coincides with T_c, and for $T > T_c$ there is never any form of stiffness [6, 11]. Before entering the asymptotic region, however, the only measure of temperature available to the PDE is the amplitude of the oscillations of $\tilde{\phi}$ at higher Q. The particularly small local extrema characteristic of the HCY fluid then effectively render the numerics at intermediate cutoff similar to what would be found only at much higher T/T_c in other systems, thus reducing the problem posed by transient stiffness there.

In case the above line of thought actually captures the feature responsible for the singular position of the default choice of HCY potential, our interest is naturally drawn to the form of $\tilde{u}_0$, and to the choice of $w(r)$ inside the core in particular: With hard spheres serving as reference system, $w(r)$ is not uniquely determined for $r < \sigma$ but nevertheless affects $\tilde{\phi}$ throughout $\mathcal{D}$. This carries over immediately to f and all the other properties of the Q system except in the limits $Q \to \infty$ and $Q \to 0$. (The necessary independence of the physically significant quantities obtained in the latter limit is actually borne out in a rather satisfactory way in some preliminary calculations on the Girifalco description of fullerenes [16].) The importance of the continuation of $w(r)$ inside the core can also be seen from the dot-dashed curve in fig. 4, corresponding to the HCY potential with $\epsilon_0 = 0$: Just as in ref. 14, any discontinuity in $w(r)$ is bound to feature prominently in the Fourier transform, and even a moderate deviation from the standard choice of $\epsilon_0 = \epsilon$ is found to render the local extrema of $\tilde{u}_0$ comparable the SW case, and furthermore to cause numerical difficulties at intermediate Q similar to those found in SWs [10, 11]. On the other hand, if we not only avoid such a discontinuity but rather extend the Yukawa form all the way to the origin — hardly an unproblematic choice in our formulation as it entails diverging direct correlation function at $r = 0$ and invalidates the expansion method of taking into account the core condition [6] —, we obtain $\tilde{u}_0(Q) = z^2/(z^2 + Q^2)$ which is positive and strictly monotonous for all Q (dotted curve in fig. 4). The properties of $\tilde{u}_0$ pointed out before and the attendant especially attractive numerical properties of HCY fluids with the standard setting of ϵ_0 thus appear merely as a result of a particular choice, shared with the original implementation, of $w(r)$ for $r < \sigma$ in eq. (3) and so are no genuine traits of this model system.

Heuristic as the considerations of this section are, not only do they provide us with an explanation on the level of the PDE for the dependence of the numerical properties of the PDE on the potential type, the form of $w(r)$ inside the core, and the interaction range but they also point to a rather special standing of the HCY potential in the usual parameterization of eq. (3). By the same token, care must be exercised when drawing general conclusions on the merits of HRT relative to those of other liquid state theories on the basis of HCY calculations alone, which should be kept in mind when interpreting the findings of ref. 15 where inverse screening lengths in the range $1.8/\sigma \leq z \leq 9/\sigma$ have been considered. The alleged influence of the form of $\tilde{\phi}$ on the severity of the numerical difficulties encountered when solving the HRT PDE also opens up the possibility of tuning the computational properties of some given potential by optimizing $w(r)$ inside the core in such a way that the local extrema are reduced in magnitude, an avenue largely unexplored to date the merit of which we are currently in no position

to assess.

With these rather informal and partly speculative considerations the present installment of this short series of reports on the character and essential features of the HRT PDE for thermodynamic states of infinite isothermal compressibility κ_T draws to an end: Building upon the analysis of part I [1], in the early sections of this report we have presented a host of numerical evidence that we deem sufficient for establishing the stiff scenario for the asymptotic solution at phase separation. On this basis we have then been able to extend some of our conclusions to similar effects at intermediate values of the cutoff Q_z and we have tentatively identified the way the form of ϕ affects the numerics there as well as in the asymptotic region. All in all, we feel that we have amassed a considerable amount of numerical experience and arrived at a rather detailed self-consistent perception of the computational process all the way from the initial conditions imposed at large Q to the final results at $Q = 0$ where the solution reproduces infinite κ_T at the critical point and at phase coexistence. Given the precarious nature of the HRT numerics and the not altogether unproblematic relation between the PDE and the FD approximation of it such an understanding is of prime importance if systematic mistakes are not to be introduced into the results unknowingly. We will strive to bring to fruition our concept of the integration of the discretized equations in part III [13] where we will also discuss the significance of our findings so far for the data analysis, an endeavour that seems all the more worthwhile in view of the high promise of HRT as one of the few theories of the liquid state that remain applicable even in the critical region.

VII. ACKNOWLEDGMENTS

The authors gratefully acknowledge financial support from *Fonds zur Förderung der wissenschaftlichen Forschung* (*Austrian Science Fund*, FWF) under project number P15758-N08.

[1] A. Reiner, *Infinite compressibility states in the hierarchical reference theory of fluids. I. Analytical considerations*, submitted to J. Stat. Phys.. Available on the world wide web from `http://purl.oclc.org/NET/a-reiner/sci/texts/20030615-0/`.

[2] A. Parola, L. Reatto, *Liquid state theories and critical phenomena*, Adv. Phys. **44**, 211–298 (1995).

[3] A. Parola, L. Reatto, *Liquid-state theory for critical phenomena*, Phys. Rev. Lett. **53**, 2417–2420 (1984).

[4] A. Parola, L. Reatto, *Hierarchical reference theory of fluids and the critical point*, Phys. Rev. A **31**, 3309–3322 (1985).

[5] A. Parola, A. Meroni, L. Reatto, *Comprehensive theory of simple fluids, critical point included*, Phys. Rev. Lett. **62**, 2981–2984 (1989).

[6] A. Meroni, A. Parola, L. Reatto, *Differential approach to the theory of fluids*, Phys. Rev. A **42**, 6104–6115 (1990).

[7] A. Parola, D. Pini, L. Reatto, *First-order phase transitions, the Maxwell construction, and the momentum-space renormalization group*, Phys. Rev. E **48**, 3321–3332 (1993).

[8] M. Tau, A. Parola, D. Pini, L. Reatto, *Differential theory of fluids below the critical temperature: Study of the Lennard-Jones fluid and of a model of C_{60}*, Phys. Rev. E **52**, 2644–2656 (1995).

[9] A. Reiner, G. Kahl, Poster presented at *5^{th} EPS Liquid Matter Conference*, Konstanz, Germany, 2002. Abstract in Europh. Conf. Abs. **26F**, 10.17 (2002). Available on the world wide web from `http://purl.oclc.org/NET/a-reiner/sci/texts/20020915-0/`.

[10] A. Reiner, G. Kahl, *Implementation of the hierarchical reference theory for simple one-component fluids*, Phys. Rev. E **65**, 046701 (2002). E-print `cond-mat/0112035`.

[11] A. Reiner, *The hierarchical reference theory. An application to simple fluids*, PhD thesis, Technische Universität Wien (2002). Available on the world wide web from `http://purl.oclc.org/NET/a-reiner/dr-thesis/`.

[12] A. Reiner, *ar-HRT-1. Implementation of the Hierarchical Reference Theory for one-component fluids.* Available on the world wide web from `http://purl.oclc.org/NET/ar-hrt-1/`.

[13] A. Reiner, G. Kahl, *Infinite compressibility states in the hierarchical reference theory of fluids III*, in preparation. Available on the world wide web from `http://purl.oclc.org/NET/a-reiner/sci/texts/20030710-0/`.

[14] A. Reiner, G. Kahl, *The hierarchical reference theory as applied to square well fluids of variable range*, J. Chem. Phys. **117**, 4925–4935 (2002). E-print `cond-mat/0208471`.

[15] C. Caccamo, G. Pellicane, D. Costa, D. Pini, G. Stell, *Thermodynamically self-consistent theories of fluids interacting through short-range forces*, Phys. Rev. E **60**, 5533–5543 (1999).

[16] L. A. Girifalco, *Interaction potential for C_{60} molecules*, J. Phys. Chem. **95**, 5370–5371 (1991).

system	$\beta_c\,\epsilon$	$\varrho_c\,\sigma^3$	$\beta\,\epsilon$	$\varrho_v\,\sigma^3$	$\varrho_l\,\sigma^3$
SW, $\lambda = 3$	0.1011	0.26(1)	0.115	0.075(5)	0.510(5)
HCY, $z = 1.8/\sigma$	0.8316	0.33(1)	0.875	0.145(5)	0.525(5)

TABLE I: Overview of systems and sample isotherms: β_c and ϱ_c give the location of the critical point, ϱ_v and ϱ_l the extent of the two-phase region at the inverse temperature β considered in the tables and figures to follow. The numbers have been obtained from HRT calculations not imposing the core condition. All of the digits indicated for β_c are significant.

$\Delta Q\big\vert_\infty\,\sigma$	$Q_{\min}\,\sigma$	$f_{0.2}$	$f_{0.2}\,Q_{\min}\,\sigma$	$F_{0.2}^{0.3}$	$F_{0.2}^{0.4}$	$F_{0.2}^{0.5}$
0.003	$9.914 \cdot 10^{-3}$	$3.643 \cdot 10^{2}$	3.612	1.862	1.755	0.590
0.004	$3.995 \cdot 10^{-5}$	$8.990 \cdot 10^{4}$	3.592	1.867	1.758	0.585
0.005	$5.014 \cdot 10^{-5}$	$7.163 \cdot 10^{4}$	3.592	1.867	1.758	0.585
0.010	$9.943 \cdot 10^{-5}$	$3.612 \cdot 10^{4}$	3.592	1.867	1.758	0.585

TABLE II: ΔQ dependence of the final results for a hard-core Yukawa system: Just as in figs. 1 and 2, $z = 1.8/\sigma$, $\beta = 0.875/\epsilon$, and $\Delta\varrho = 10^{-2}/\sigma^3$; we use the notation f_x for $f(Q_{\min}, x/\sigma^3)$ and define $F_x^y = f_y/f_x$.

$\Delta Q\big\vert_\infty\,\sigma$	$G_{0.2}$	$G_{0.3}$	$G_{0.4}$	$G_{0.5}$
0.003	1.011	1.013	1.018	1.072
0.004	1.017	1.016	1.022	1.087
0.005	1.017	1.016	1.022	1.086
0.010	1.017	1.016	1.022	1.086

TABLE IV: $\Delta\varrho$ dependence of the form of the final results for a hard-core Yukawa system at varying ΔQ: The parameters coincide with those of tabs. II and III; perusing the notation introduced there, G_x is $f_x\,Q_{\min}\,\sigma$ as evaluated for $\Delta\varrho = 5 \cdot 10^{-4}/\sigma^3$ divided by the same quantity for $\Delta\varrho = 10^{-2}/\sigma^3$.

$\Delta Q\big\vert_\infty\,\sigma$	$Q_{\min}\,\sigma$	$f_{0.15}$	$F_{0.15}^{0.25}$	$F_{0.25}^{0.35}$	$F_{0.35}^{0.45}$
0.003	$4.181 \cdot 10^{-4}$	$-1.415 \cdot 10^{5}$	2.379	1.635	0.392
0.004	$3.198 \cdot 10^{-4}$	$3.597 \cdot 10^{4}$	1.589	0.965	0.523
0.005	$3.318 \cdot 10^{-4}$	$3.465 \cdot 10^{4}$	1.589	0.965	0.523
0.010	$3.576 \cdot 10^{-4}$	$3.225 \cdot 10^{4}$	1.589	0.965	0.523

TABLE V: ΔQ dependence of the final results for a SW system with $\lambda = 3$, $\beta = 0.115/\epsilon$, and $\Delta\varrho = 10^{-2}/\sigma^3$; we use the same notation as in tab. II.

$\Delta Q\big\vert_\infty\,\sigma$	$Q_{\min}\,\sigma$	$f_{0.15}$	$F_{0.15}^{0.25}$	$F_{0.25}^{0.35}$	$F_{0.35}^{0.45}$
0.003	$4.206 \cdot 10^{-4}$	$2.812 \cdot 10^{4}$	1.584	0.974	0.547
0.004	$3.302 \cdot 10^{-4}$	$3.589 \cdot 10^{4}$	1.584	0.974	0.547
0.005	$3.318 \cdot 10^{-4}$	$3.551 \cdot 10^{4}$	1.584	0.974	0.547
0.010	$3.685 \cdot 10^{-4}$	$3.178 \cdot 10^{4}$	1.589	0.974	0.545

TABLE VI: ΔQ dependence of the final results for a SW system: The parameters and notation coincide with those of tab. V, except for $\Delta\varrho = 5 \cdot 10^{-4}/\sigma^3$.

$\Delta Q\big\vert_\infty\,\sigma$	$Q_{\min}\,\sigma$	$f_{0.2}$	$f_{0.2}\,Q_{\min}\,\sigma$	$F_{0.2}^{0.3}$	$F_{0.2}^{0.4}$	$F_{0.2}^{0.5}$
0.003	$3.131 \cdot 10^{-5}$	$1.167 \cdot 10^{5}$	3.652	1.865	1.768	0.625
0.004	$1.004 \cdot 10^{-2}$	$3.638 \cdot 10^{2}$	3.653	1.865	1.768	0.625
0.005	$5.014 \cdot 10^{-5}$	$7.285 \cdot 10^{4}$	3.652	1.865	1.768	0.625
0.010	$1.004 \cdot 10^{-4}$	$3.637 \cdot 10^{4}$	3.653	1.865	1.768	0.625

TABLE III: ΔQ dependence of the final results for a hard-core Yukawa system: The parameters and notation coincide with those of tab. II, except for $\Delta\varrho = 5 \cdot 10^{-4}/\sigma^3$.

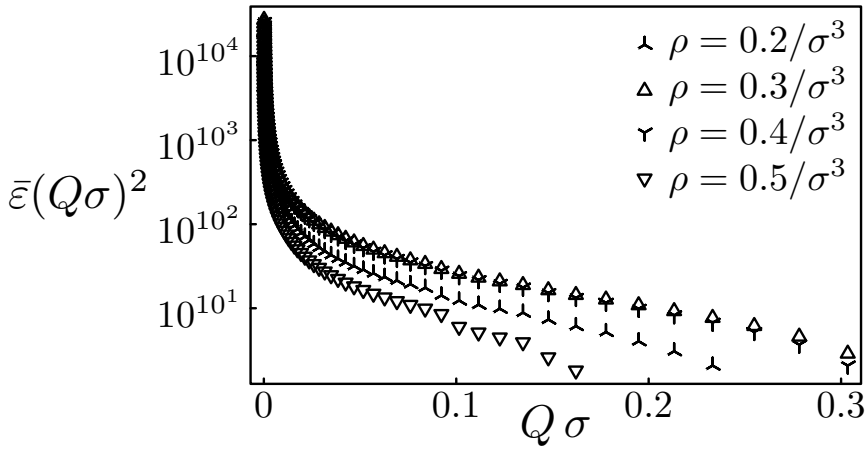

FIG. 1: $\bar{\varepsilon}\,Q^2$ as a function of Q for various densities inside the binodal: The data have been obtained for a hard-core Yukawa potential with inverse screening length $z = 1.8/\sigma$ and for an inverse temperature of $\beta = 0.875/\epsilon$; the numerical precision in the calculations was $\epsilon_{\#} = 10^{-2}$, the step size for infinite cutoff was $\Delta Q\Big|_{\infty} = 10^{-2}/\sigma$.

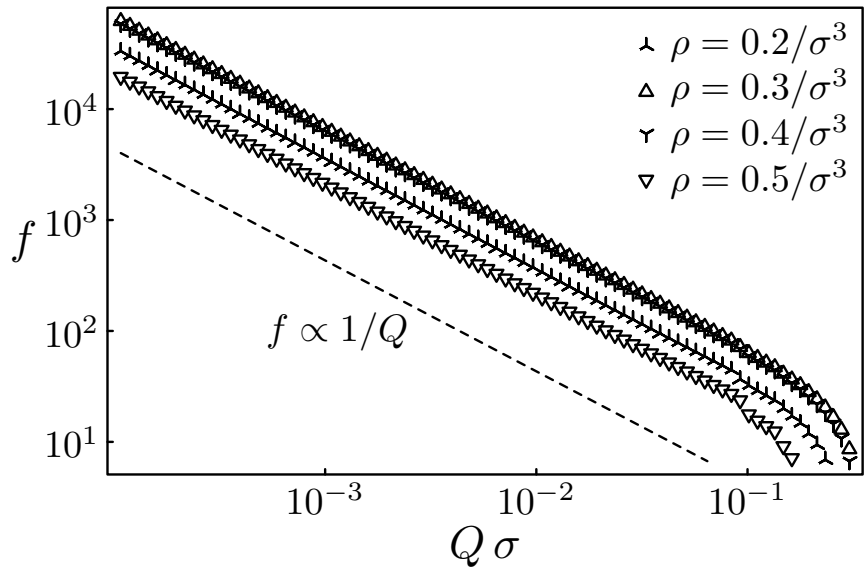

FIG. 2: f as a function of Q for various densities inside the binodal: The data have been obtained for the same hard-core Yukawa potential and with the same numerical parameters as in fig. 1. The dashed line indicates the slope corresponding to proportionality of f to the reciprocal of the cutoff; subsequent symbols are separated by ten steps in the $-Q$ direction.

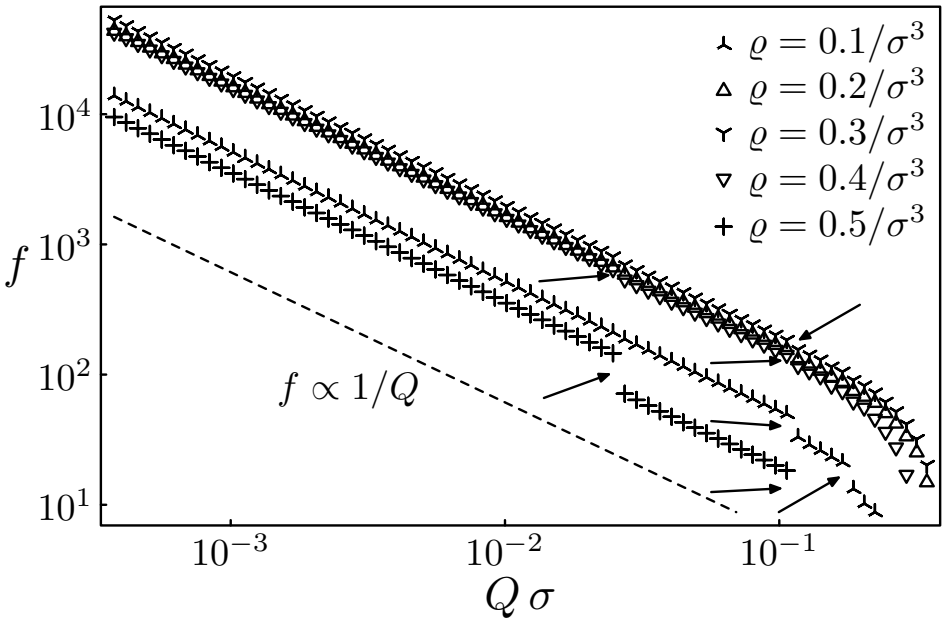

FIG. 3: f as a function of Q for various densities inside the binodal: The data have been obtained for a SW potential with $\lambda = 3$ and at a temperature of $\beta = 0.115/\epsilon$; otherwise, the remarks of fig. 2 apply. Arrows mark several of the near-discontinuities discussed in section III C.

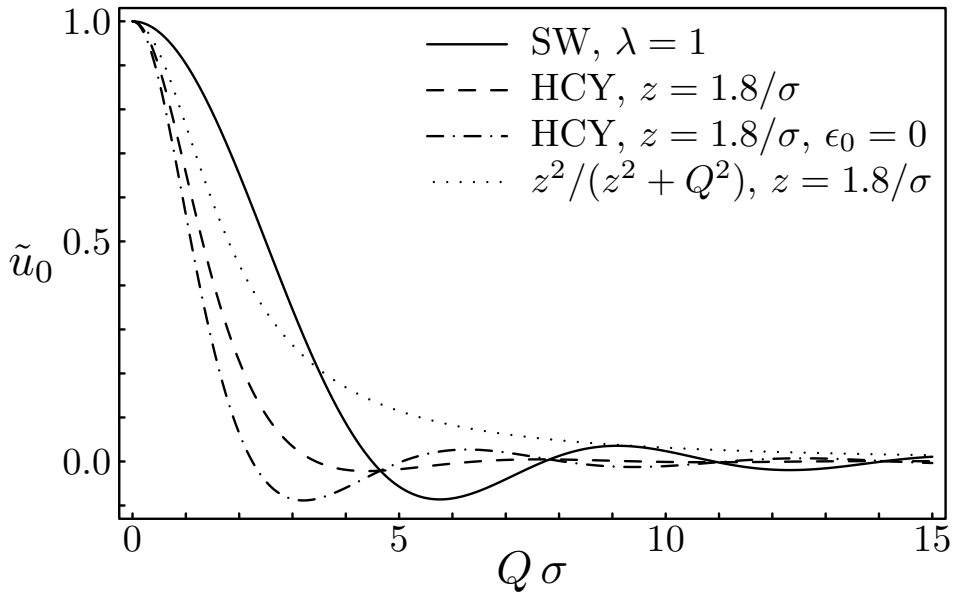

FIG. 4: $\tilde{u}_0$ as a function of Q for SW and HCY potentials with the parameters indicated: If, contrary to eq. (3), the Yukawa form is retained even inside the core, $\tilde{u}_0(Q)$ is given by $z^2/(z^2+Q^2)$. As far as the SW potential is concerned, λ and Q enter $\tilde{u}_0$ only in the combination λQ so that a variation of the potential range only introduces a linear rescaling of the Q dependence of the function. We have checked that the graph remains qualitatively unchanged for different parameter settings. The first minimum of $\tilde{u}_0$ is -0.02 for the default HCY potential, -0.09 for the HCY potential with $\epsilon_0 = 0$, and slightly above -0.09 for the SW potential.

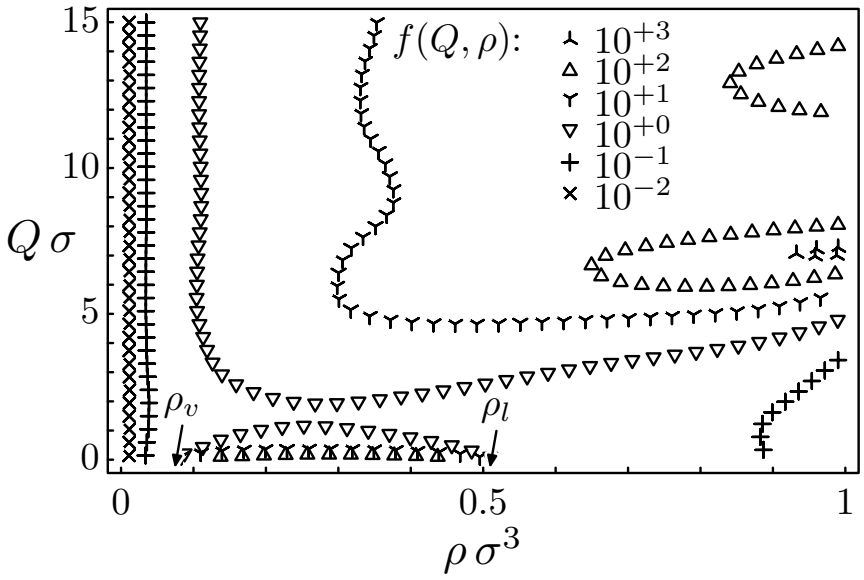

FIG. 5: $f(Q, \varrho)$ for intermediate cutoff as a logarithmic contour plot: The data has been obtained for SWs with $\lambda = 3$ at inverse temperature $\beta = 1/k_B\,T = 0.115/\epsilon$. Both the approach to the low-density boundary condition of vanishing f at densities below $0.01/\sigma^3$ and the final build-up of infinite compressibility at cutoffs below $10^{-1}/\sigma$ have been excluded from the graph.